treated groups (bimosiamose 45.7 ± 2.9%; vehicle 46.7 ± 3.0%). In contrast, infarct/area at risk was significantly different between bimosiamose- and vehicle-treated groups after 24 h of reperfusion (bimosiamose 29.8 ± 5.7%; vehicle 50.7 ± 4.2%; $P = 0.01$). Bimosiamose also significantly decreased Infarct/LV compared to the vehicle-treated group (bimosiamose 11.8 ± 2.0%; vehicle 26.1 ± 3.5%; $P < 0.01$) (Fig. 2C).

3.2. Bimosiamose prevents myocardial dysfunction after infarction

As a baseline, normal M-mode echocardiograms were obtained from age- and weight-matched rats and their average baseline of %FS was 47.4 ± 1.9% (Fig. 3A). Fig. 3B is a representative M-mode echocardiogram of the vehicle-treated rat after 24 h of reperfusion showing that the wall motion in antero-lateral region of left ventricle is decreased remarkably. However, bimosiamose improved the regional wall motion in rat after 24 h of reperfusion (Fig. 3C). Serial change of %FS is presented in Fig. 3D. There was no difference in %FS at baseline and at immediately after ischemia/reperfusion between the bimosiamose- and the vehicle-treated groups. However, after 24 h of reperfusion, %FS of the bimosiamose-treated group was improved significantly compared to the vehicle-treated group (bimosiamose 39.9 ± 1.8%; vehicle 25.7 ± 1.6%; $P < 0.001$). Sham-operated group showed no significant change in cardiac function though serial echocardiographic measurements.

3.3. Bimosiamose reduces myocardial polymorphonuclear neutrophils accumulation

The number of polymorphonuclear neutrophils infiltrating into the area at risk of the reperfused myocardium was reduced obviously in the bimosiamose-treated rats. Significantly fewer polymorphonuclear neutrophils were found in the bimosiamose-treated hearts compared to the vehicle-treated hearts (bimosiamose 11.0 ± 2.6 vs. vehicle 23.2 ± 1.6/high-powered field; $P < 0.005$) (Fig. 4A). Myeloperoxidase activity was very low in the area not at risk myocardium of each group, however, was increased remarkably in the area at risk myocardium of the vehicle-treated hearts. Ischemia/reperfusion-induced myeloperoxidase activity was reduced significantly in the heart tissue of area at risk by treatment with bimosiamose as shown in Fig. 4B. Reduction rate was 78% compared to the vehicle-treated group ($P < 0.0001$).

3.4. Bimosiamose inhibits neutrophil rolling and adhesion under physiological flow conditions

Very few rolling or adherent HL-60 cells were observed when unactivated human umbilical vein endothelial cell (without Interleukin-1β stimulation) were used, and

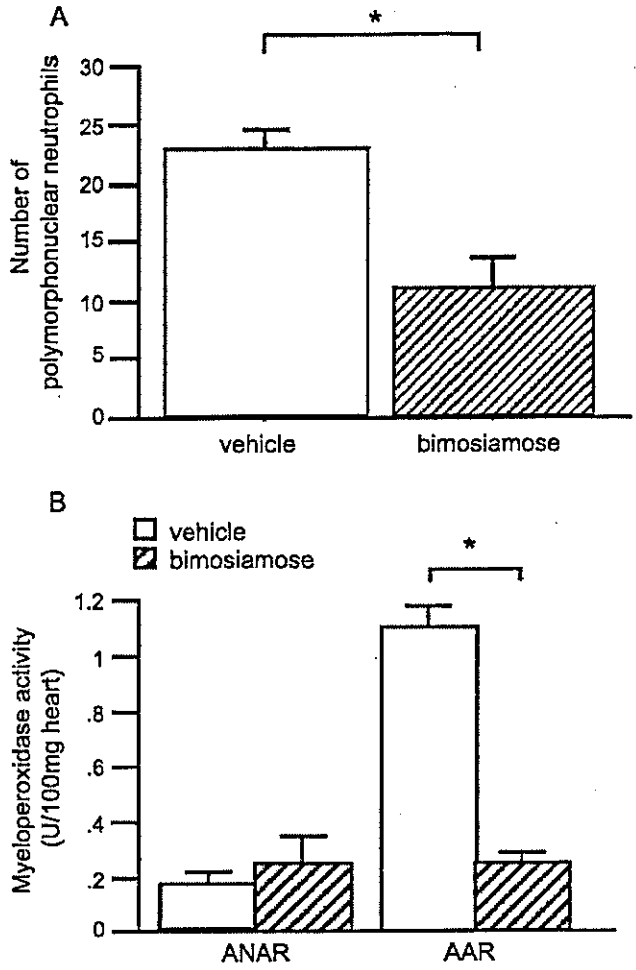

Fig. 4. (A) Average numbers of infiltrating polymorphonuclear neutrophils per × 400 field in the myocardium collected from bimosiamose-treated rats ($n = 5$) and vehicle-treated rats ($n = 5$). Polymorphonuclear neutrophils were counted in five fields of each heart and averaged. *$P < 0.005$ compared with rat given vehicle. (B) Myocardial myeloperoxidase activity in area at risk (AAR) and area not at risk (ANAR) cardiac tissue samples obtained from vehicle- and bimosiamose-treated rats. **$P < 0.0001$ compared with rat given vehicle.

similar results were obtained when unactivated human umbilical vein endothelial cells were incubated with bimosiamose (100 μM, 30 min) or vehicle (100 μM, 30 min). However, the number of HL-60 cells that showed rolling and adhesion to human umbilical vein endothelial cells was increased significantly after cytokine-activation (Interleukin-1β, 20 U/ml, 4 h), and similar degree of increase in HL-60 cells interactions was observed when activated human umbilical vein endothelial cells were pretreated with vehicle (Fig. 5A). In contrast, pretreatment with bimosiamose reduced remarkably the number of HL-60 cells that interacted with activated human umbilical vein endothelial cells (Fig. 5B). Reduction rate was significant in both rolling (62%, $P < 0.001$) and adhesion (38%, $P < 0.05$), when 100 μM of bimosiamose was used, compared with the vehicle-pretreatment cells as shown in Fig. 5C and D. The

Available online at www.sciencedirect.com

SCIENCE DIRECT

Life Sciences 75 (2004) 1333–1341

Life Sciences

www.elsevier.com/locate/lifescie

MCP-1-induced enhancement of THP-1 adhesion to vascular endothelium was modulated by HMG-CoA reductase inhibitor through RhoA GTPase-, but not ERK1/2-dependent pathway

Megumi Hiraoka[a,1], Noriko Nitta[a,1], Miyudzu Nagai[b], Kentaro Shimokado[b], Masayuki Yoshida[a,b,*]

[a] *Department of Medical Biochemistry, Graduate School of Medicine, Tokyo Medical and Dental University, Tokyo, Japan*
[b] *Department of Vascular Medicine, Graduate School of Medicine, Tokyo Medical and Dental University, Tokyo, Japan*

Received 21 July 2003; accepted 24 February 2004

Abstract

Monocyte-endothelial interaction plays a pivotal role in atherosclerosis. We previously showed that HMG CoA reductase inhibitor reduces adhesion, however, not the rolling of monocytes to vascular endothelium under flow in vitro. In the present study, we investigated the effect of pitavastatin, a novel HMG CoA reductase inhibitor, on the transition from monocyte rolling on vascular endothelium to stable adhesion induced by MCP-1 under flow (shear stress = 1.0 dyne/cm^2). Control THP-1 cells rolled on activated (IL-1β, 4 hours) human umbilical vein endothelial cells (HUVEC) and the number of adhered THP-1 cells were significantly enhanced following the addition of 50 nM of MCP-1 ($p < 0.002$). In contrast, MCP-1 failed to convert pitavastatin-treated (10 μM, 48 hours) THP-1 rolling to stable adhesion, as compared to baseline adhesion, prior to the addition of MCP-1 ($p > 0.4$). Pitavastatin-induced changes in THP-1 cells were reversed by treatment with 10 μM of mevalonate, the intermediate of cholesterol biosynthesis. To elucidate the mechanism by which pitavastatin modulates MCP-1-induced THP-1 adhesive interactions, the possible involvement of extracellular signal-regulated kinase 1/2 (ERK1/2) was examined. Western blotting analysis using an anti-ERK1/2 Ab and an antibody against phosphorylated-ERK1/2 (p-ERK) revealed that pitavastatin treatment significantly inhibited the MCP-1-induced phosphorylation of ERK1/2. Further, a RhoA pull-down assay revealed that activation of RhoA GTPase was reduced after pitavastatin treatment. Interestingly, an inhibitor of RhoA GTPase, but not that of the ERK1/2 pathway, attenuated MCP-1-dependent adhesion of THP-1 cells to HUVEC. These findings indicate a role for pitavastatin in modulating the

* Corresponding author. Department of Medical Biochemistry, Tokyo Medical and Dental University, 1-5-45, Yushima Bldg. D-256, Bunkyo, Tokyo 113-8519, Japan. Tel.: +81-3-5803-5228; fax: +81-3-5800-3380.
E-mail address: masavasc@tmd.ac.jp (M. Yoshida).
[1] These two authors contributed equally to this work.

doi:10.1016/j.lfs.2004.02.028

MCP-1-induced phenotypic changes of monocyte-endothelial interactions, which may account for the anti-inflammatory effects of statins.

Keywords: HMG CoA reductase inhibitor; MCP-1; Monocytes; Atherosclerosis

Introduction

Recently, 3-hydroxyl-3-methylglutaryl (HMG)-CoA reductase inhibitors (statins) have been shown to decrease the occurrence of myocardial infarction and other ischemic vascular events in hyperlipidemic individuals by lowering the plasma level of LDL-cholesterol (4S Group, 1994). Interestingly, several clinical trials have suggested that statins might also have beneficial effects that are independent from their cholesterol-lowering actions (Shepherd et al., 1995). Our group recently examined the inhibitory effect of statins on monocyte-endothelial adhesion under flow (Yoshida et al., 2001) and showed that the adhesion of monocytes to vascular endothelium is one of the crucial steps in atherogenesis. Circulating monocytes first roll on vascular endothelium primarily via a selectin-dependent interaction, which is followed by stable adhesion to the surface of the endothelium.

Although numerous reports have described the importance of adhesion molecules, there is little information on the dynamic transition from rolling to stable adhesion. In the present study, we characterized the effect of pitavastatin on the transition of monocytes from rolling to stable adhesion using THP-1 cells in a previously described flow chamber. We discovered that the incubation of THP-1 cells in the presence of pitavastatin significantly inhibited the transition from rolling to stable adhesion, which resulted in an aberrant adhesive interaction. We also elucidated the possible involvement of RhoA inactivation following treatment with pitavastatin. Our results further support the hypothesis that statins have pleiotropic effects and may contribute to establishment of a novel therapeutic approach for inflammatory vascular diseases.

Methods

Cell culture and reagents

Human umbilical vein endothelial cells (HUVEC) were isolated from normal-term umbilical veins and cultured in 0.1% gelatin-coated tissue culture dishes as described previously (Yoshida et al., 1996, 2001) in RPMI-1640 supplemented with 20% FCS (Life Technologies Oriental Inc., Tokyo), endothelial growth factor (25 μg/ml, Funakoshi Co. Ltd., Tokyo, Japan), porcine intestinal heparin (50 μg/ml, Sigma-Aldrich JAPAN, K.K., Tokyo), penicillin, and streptomycin. The THP-1 cell line (American Type Culture Collection, (Rockville, MD) was cultured in RPMI-1640 containing 10% FCS. For use in the flow chamber apparatus, HUVEC (passages 2 and 3) were plated on 22-mm fibronectin-coated glass cover slips, as previously described (Yoshida et al., 2001). Recombinant human IL-1â was obtained from Genzyme (Cambridge, MA). BCECF-AM and FITC-phalloidin were purchased from Molecular Probes (Eugene, OR). Pitavastatin, a kind gift from Kowa Inc. (Tokyo), was stored as a 10-mM stock solution in DMSO. Mouse anti-RhoA mAb was purchased from Santa Cruz Biotechnology Inc. (Santa Cruz, CA)

and a mouse anti-CCR2 antibody (clone 48607.211) was obtained from Genzyme-Techne MN). Anti-extracellular signal regulated kinase (ERK)1/2 and anti-phospho-ERK1/2 (Thr202/Tyr204) were obtained from New England Biolabs (Beverly, MA).

Adhesion assay under laminar flow

The parallel-plate flow chamber used in the present study has been previously described in detail (Yoshida et al., 2001; Kawakami et al., 2002). Endothelial monolayers on coverslips were stimulated with IL-1â (10 u/ml) for 4 hours and positioned in the flow chamber, which was mounted on an inverted microscope. Each monolayer was perfused for 5 minutes with perfusion medium and then examined carefully to verify confluence. Next, THP-1 cells, pre-treated with pitavastatin, were added to the perfusion medium at a cell density of 10^6 cells/ml. The THP-1 cells were drawn through the chamber at controlled flow rates to generate a calculated wall shear stresses of 1.0 dyne/cm^2 for 10 minutes. The entire period of perfusion was recorded on videotape using a digital video recorder with a time generator. Where indicated, MCP-1 was added to the THP-1 cells in the perfusion media just prior to the assay. Captured images were then transferred to a computer for image analysis to determine the number of rolling and adherent THP-1 cells in 5 to 10 randomly selected 20 × microscope fields during the final minute of each experiment.

Flow cytometric analysis

THP-1 cells were incubated with the indicated primary antibodies for 45 minutes on ice, washed twice with RPMI1640 containing 5% FCS, and then incubated with an FITC-tagged goat anti-mouse antibody (Caltag, Burlingame, CA). Fluorescence was analyzed using a FACSCaliber (Becton-Dickinson, San Jose, CA).

RT–PCR

Cytoplasmic RNA was isolated from the cells in TRIZOL reagent according to the manufacturer's recommendations (Invitrogen). First-strand DNA was synthesized using reverse transcriptase with random hexamers from 1 μg of total RNA in a 20-μL reaction volume according to the manufacturer's protocol (GeneAmp RNA PCR Kit; Perkin-Elmer), then one-tenth of the resulting reverse transcription (RT) product was applied to each 25-μL PCR solution. Primers were synthesized from reported sequences and yielded products of 221 bp (forward, 5′-CTGTGTTTGCTTCTGTCCCAGG-3′, reverse, 5′-TGCCCTATGCCTCTTCTTCTCG-3′, human CCR2) and 353 bp (forward, 5′-GCTCGTCGTCGA-CAACGGCTC-3′, reverse, 5′-CAAACATGATCTGGGTCATCTTCTC-3′, human β-actin) in length. Polymerase chain reaction (PCR) products (10 μL) were subjected to 1.5% agarose gel electrophoresis and stained with ethidium bromide. The intensity of each band was quantitated using an LAS1000 image analyzer (Fuji Film).

Western blotting

THP-1 cells were cultured in the presence of pitavastatin for 48 hours, after which they were lysed and the cell lysate was collected, as described previously (Yoshida et al., 2001). An equal amount of

protein (10 μg) from each condition was subjected to 12.5% SDS–PAGE. Western blotting was carried out using the indicated primary antibodies followed by incubation with a secondary IgG conjugated to HRP. Immunoreactive proteins were detected using an enhanced chemiluminescence (ECL) kit (Amersham Pharmacia Biotech, IL). Activation of RhoA was determined using a GST-fusion protein from the Rho binding domain of the Rho effector Rhotekin (Rho Activation Assay Kit, Upstate Biotechnology, NY) following the manufacturer's protocol.

Statistical tests

Results are presented as mean ± S.D. Data were analyzed using analysis of variance (ANOVA), with $P < 0.05$ considered significant.

Results

Pitavastatin reduces transition of THP-1 cells from rolling to adhesion under laminar flow conditions

First, we observed the effects of pitavastatin on the adhesion of THP-1 cells to vascular endothelium. As previously reported (Yoshida et al., 2001), THP-1 cells predominantly adhered to activated HUVEC, while pretreatment with pitavastatin (10 μM, 48 hours) significantly reduced the number of adhered cells (Fig. 1). When MCP-1 was added to the THP-1 cells, the number of adhered cells increased ($p < 0.002$). In contrast, pretreatment with pitavastatin significantly inhibited the enhanced adhesion elicited by MCP-1 ($p > 0.4$, N.S.). In addition, co-incubation with pitavastatin and mevalonate (10 μM) cancelled the effect of pitavastatin. These effects of pitavastatin were observed at a concentration as low as 1.0 μM and required a preincubation period of at least 24 hours (data not shown).

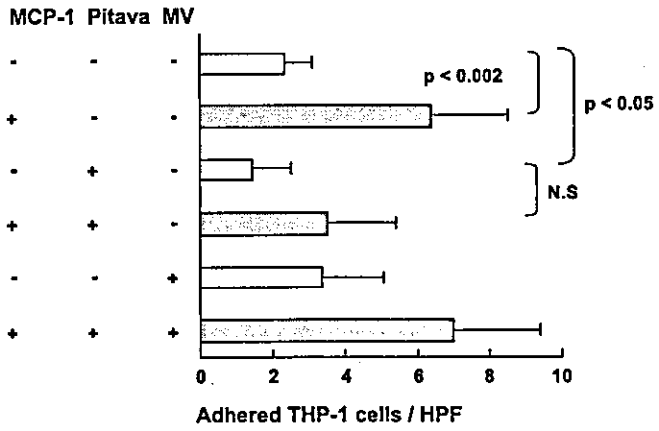

Fig. 1. Effects of pitavastatin on MCP-1-induced THP-1 cell adhesion to vascular endothelium. THP-1 cells were incubated in the presence or absence of 10 μM of pitavastatin (Pitava) for 48 hours, and then an adhesion assay under laminar flow was carried out in the presence or absence of MCP-1 (50 ng/ml), added just prior to the assay, as described in Methods. In some experiments, THP-1 cells were incubated in the presence of both mevalonic acid (MV) (10 μM) and pitavastatin for 48 hours. Data are representative of 4 similar experiments.

Pitavastatin and CCR2 expression inTHP-1 cells

To elucidate the potential mechanism involved in the observed phenomenon, THP-1 cells were subjected to flow cytometry. As shown in Fig. 2A, the expression of CCR2 on the cell surface decreased after pitavastatin treatment, though not dramatically (10 μM, 48 hours). Further, semi-quantitative RT-PCR analysis revealed that CCR2 was not significantly altered at the message level following pitavastatin treatment (Fig. 2B).

Pitavastatin reduces MCP-1-induced activation of ERK1.2 and Rho AGTPase

It has been reported that ERK activation is involved in MCP-1-mediated THP-1 integrin activation (Ashida et al., 2001), therefore, we examined the effect of pitavastatin on MCP-1-mediated ERK activation. As shown in Fig. 3, MCP-1 induced phosphorylation of ERK protein in THP-1 cells.

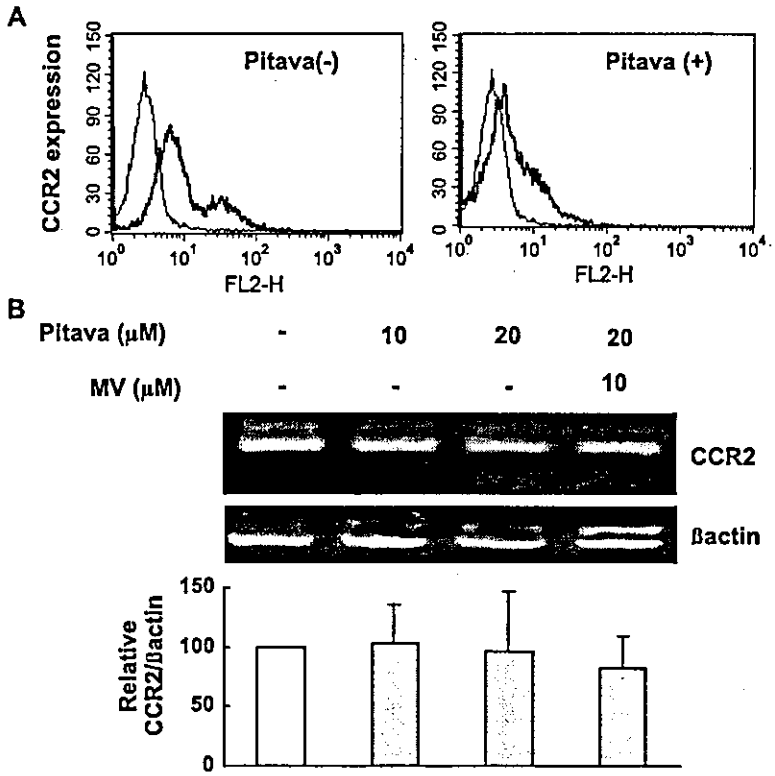

Fig. 2. Flow cytometric analysis of THP-1 cells before and after pitavastatin treatment. (A) THP-1 cells were pre-incubated in the absence (−) or presence (+) of 10 μM of pitavastatin (Pitava) for 48 hours, and then CCR2 expression (bold line) was detected using anti-CCR2 mAb followed by FITC-labeled anti-mouse polyclonal IgG and compared to non-binding IgG (thin line). (B) THP-1 cells were pre-incubated in the presence of the indicated amounts of pitavastatin (Pitava) for 48 hours, after which total RNA was recovered and cDNA was prepared. A semi-quantitative PCR assay was carried out using primers specific for MCP-1 and β actin, as described in Methods. PCR products were subjected to 1.5% agarose electrophoresis to detect cDNA. The intensity of each band was quantitated using an LAS1000 image analyzer and the results of 3 independent experiments are summarized as a Bar graph. There were no significant differences between the columns.

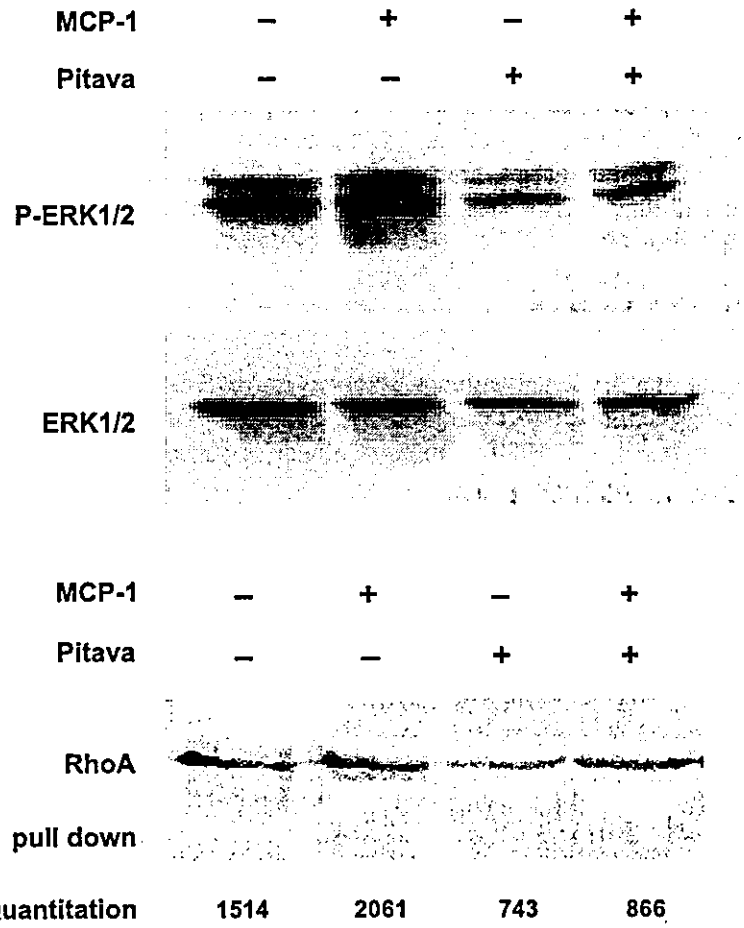

Fig. 3. Involvement of ERK1/2 and RhoA in MCP-1-induced THP-1-adhesion to vascular endothelium. THP-1 cells were incubated in the absence (–) or presence (+) of pitavastatin (Pitava, 10 μM, 48 hours) with or without stimulation by MCP-1 (50 ng/ml, 5–10 minutes). Total cell lysates were prepared and subjected to Western blot analysis, using antibodies against ERK1/2 and phopho-ERK1/2 antibodies, or captured with Rhotekin beads, and blotted using the anti-RhoA antibody, as described in Methods. The intensity of each band was quantitated using an LAS1000 image analyzer. Data shown are representative of 3 independent experiments.

However, when THP-1 cells were incubated in the presence of pitavastatin for 48 hours, the MCP-1-induced phosphorylation of ERK was significantly reduced (Fig. 3A). We also examined the involvement of RhoA GTPase in this phenomenon and found that not only resting, but also MCP-1 dependent activation of RhoA were reduced following pitavastatin treatment, based on Quantitative analysis of our pull-down assay results with Rhotekin beads (Fig. 3B).

Inhibition of RhoA GTPase, but not that of ERK1/2, reduced MCP-1-induced adhesion of THP-1 cells

To determine the potential role of Rho GTPase in the phenomenon, we treated THP-1 cells with clostridium botulinum C3 ADP-ribosyltransferase, a bacterial exoenzyme known to inactivate Rho

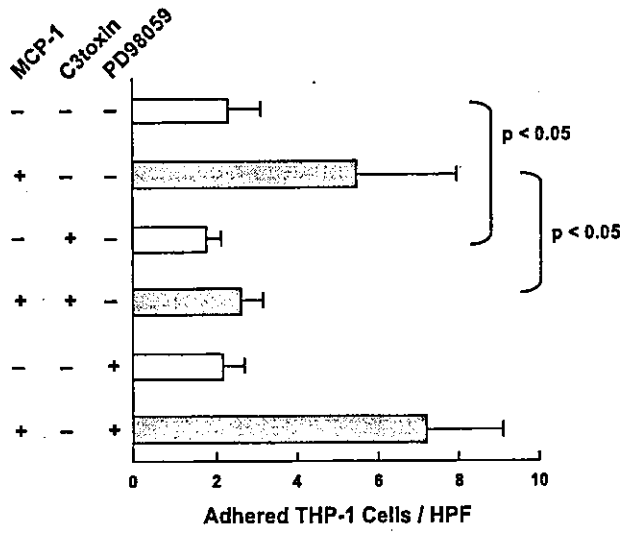

Fig. 4. Involvement of RhoA GTPase, but not of ERK1/2, in MCP-1-induced THP-1 adhesion to vascular endothelium. THP-1 cells were incubated in the presence of C3 exoenzyme (C3 toxin, 30 μg/ml, 48 hours) or PD98059 (10 μM, 4 hours) and an adhesion assay under flow was carried out in the presence or absence of MCP-1 (50 ng/ml), which was added just prior to the assay, as described in Methods. Data shown are representative of 4 independent experiments.

proteins in monocytic cells (Yoshida et al., 2001), for 48 hours at a concentration of 30 μg/ml. As shown in Fig. 4, treatment with the C3 exoenzyme for 48 hours resulted in a reduced number of adhered THP-1 cells following MCP-1 treatment ($p < 0.05$ vs. control THP-1). These effects of C3 toxin are in good agreement with our results from the RhoA pull-down assay shown in Fig. 3, thus confirming the importance of RhoA in MCP-1-dependent monocyte adhesion to endothelium. To further examine the role of ERK-dependent signalling in the MCP-1-induced enhanced adhesion of THP-1 cells, the cells were pre-treated with PD98059, a potent ERK kinase (MEK) inhibitor, prior to the adhesion assay. Interestingly, treatment with PD98059 failed to block the MCP-1-dependent THP-1 adhesion to HUVEC (Fig. 4).

Discussion

The accumulation of monocytes on vascular endothelium has been shown to be one of the earliest manifestations of atherosclerosis (Munro and Cotran, 1988). Previous pathological studies clearly demonstrated monocyte accumulation in aortic segments, even in the absence of lipid deposition (Cybulsky and Gimbrone, 1991). Further, a potential role for adhesion molecules and chemokines in atherosclerosis (Ashida et al., 2001) has been recently reported.

A previous study (Gerszten et al., 1999) used an in vitro adhesion assay performed under laminar flow conditions and revealed the dynamic role of MCP-1 in the transition from rolling to stable adhesion to vascular endothelium. Statins have been used to treat patients with hyperlipidemia, a major risk factor of atherosclerosis, because of their effects on cholesterol synthesis via the inhibition of the mevalonate pathway in the liver. However, recent observations have revealed that statins might exert lipid-independent effects in atherosclerosis. In addition, we recently demonstrated that treatment with statins

significantly reduced U937 cells adhesion, but not rolling, on activated HUVEC (Yoshida et al., 2001). In the present study, we found that treatment of THP-1 cells, from a monocytic cell line, with pitavastatin, a potent new HMG-CoA reductase inhibitor, significantly reduced the conversion from rolling to stable arrest on activated HUVEC under laminar flow conditions. This effect of pitavastatin on the transition of monocytes from rolling to adhesion was concentration-dependent (data not shown) and abrogated by simultaneous treatment with mevalonic acid.

It has been previously reported that treatment with statins reduces RhoA GTPase activation, thereby diminishing monocyte stable adhesion to vascular endothelium (Yoshida et al., 2001). The present findings extend the role of statin in modulation of the MCP-1-dependent conversion of THP-1 cells from rolling to stable adhesion, as well as subsequent signalling in THP-1 cells. Our results showed that slight reduction of CCR2 protein expression on the surface of THP-1 cells by pitavastatin, although its mRNA levels remained unchanged after pitavastatin treatment (Fig. 2A, B). These divergent effects of pitavastatin on mRNA and protein of CCR2 may require further investigation including potential changes in mRNA stability of CCR2. It was previously demonstrated that statin modulated the expression levels of adhesion molecules in monocytes following interferon γ-dependent signal transduction in an endothelial-like cell line (Chung et al., 2002), however, the observed reduction of CCR2 expression as shown in Fig. 2 does not fully explain the dramatic reduction of adhesion. Interestingly, in the present assay conditions, inhibition of RhoA, but not of ERK-1/2, reduced MCP-1-mediated THP-1 cell adhesion, suggesting that RhoA and ERK-1/2 independently regulate MCP-1-mediated signals in THP-1 cells, while RhoA GTPase plays a predominant role in the enhancement of adhesion induced by MCP-1. Although the importance of ERK-1/2 was stressed in a previous study (Ashida et al., 2001), we failed to find a relationship between ERK activation and MCP-1-dependent adhesion of THP-1 cells under our assay conditions. We utilized a well defined simulated flow chamber apparatus in an attempt to mimic monocyte recruitment that occurs in vivo, whereas that study individually observed cell adhesion under static conditions as well as chemotaxis using a Boyden chamber to determine specific intracellular signaling. These differences in experimental settings must be taken into account to fully understand the complex nature of monocyte recruitment to vascular endothelium in inflammation and atherosclerosis.

In conclusion, we demonstrated that treatment with statins dramatically reduced monocytic THP-1 cell conversion from rolling to adhesion induced by MCP-1 through the RhoA-dependent pathway. Our results suggest an anti-inflammatory role for pitavastatin.

Acknowledgements

This study was supported by Special Coordination Funds from the Ministry of Education, Science, Sports and Culture of Japan, and a grant-in-aid from the Ministry of Health, Labour and Welfare of Japan.

References

4S Group, 1994. Randomized trial of cholesterol lowering in 4444 patients with coronary heart disease: The Scandinavian Simvastatin Survival Study (4S). Lancet 344, 1383–1389.

Ashida, N., Arai, H., Yamasaki, M., Kita, T., 2001. Distinct signaling pathways for MCP-1-dependent integrin activation and chemotaxis. Journal of Biological Chemistry 276, 16555–16560.

Chung, H.K., Lee, I.K., Kang, H., Suh, J.M., Kim, H., Park, K.C., Kim, D.W., Kim, Y.K., Ro, H.K., Shong, M., 2002. Statin inhibits interferon-gamma-induced expression of intercellular adhesion molecule-1 (ICAM-1) in vascular endothelial and smooth muscle cells. Exp Mol Med 34, 451–461.

Cybulsky, M.I., Gimbrone Jr., M.A., 1991. Endothelial expression of a mononuclear leukocyte adhesion molecule during atherogenesis. Science 251, 788–791.

Gerszten, R.E., Garcia-Zepeda, E.A., Lim, Y.C., Yoshida, M., Ding, H.A., Gimbrone Jr., M., Luster, A.D., Luscinskas, F.W., Rosenzweig, A., 1999. MCP-1 and IL-8 trigger firm adhesion of monocytes to vascular endothelium under flow conditions. Nature 398, 718–723.

Kawakami, A., Tanaka, A., Nakajima, K., Shimokado, K., Yoshida, M., 2002. Atorvastatin attenuates remnant lipoprotein-induced monocyte adhesion to vascular endothelium under flow conditions. Circulation Research 91, 263–271.

Munro, J.M., Cotran, R.S., 1988. The pathogenesis of atherosclerosis: atherogenesis and inflammation. Laboratory Investigation 58, 249–261.

Shepherd, J., Cobbe, S.M., Ford, I., Isles, C.G., Lorimer, A.R., MacFarlane, P.W., McKillop, J.H., Packard, C.J., 1995. Prevention of coronary heart disease with pravastatin in men with hypercholesterolemia. West of Scotland Coronary Prevention Study Group. New England Journal of Medicine 333, 1301–1307.

Yoshida, M., Westlin, W.F., Wang, N., Ingber, D.E., Rosenzweig, A., Resnick, N., Gimbrone Jr., M., 1996. Leukocyte adhesion to vascular endothelium induces E-selectin linkage to the actin cytoskeleton. Journal of Cell Biology 133, 445–455.

Yoshida, M., Sawada, T., Ishii, H., Gerszten, R.E., Rosenzweig, A., Gimbrone Jr., M.A., Yasukochi, Y., Numano, F., 2001. HMG-CoA reductase inhibitor modulates monocyte-endothelial cell interaction under physiological flow conditions in vitro: Involvement of rho gtpase-dependent mechanism. Arteriosclerosis Thrombosis and Vascular Biology 21, 1165–1171.

E-Selectin Blockade Decreases Adventitial Inflammation and Attenuates Intimal Hyperplasia in Rat Carotid Arteries After Balloon Injury

Ryo Gotoh, Jun-ichi Suzuki, Hisanori Kosuge, Tsunekazu Kakuta, Shinji Sakamoto, Masayuki Yoshida, Mitsuaki Isobe

Objective—Inflammation is one of the initial repair processes after vascular injury. E-selectin facilitates adherence of leukocytes to vascular endothelium at the site of inflammation. Because the role of E-selectin in this process is not fully understood, we studied the role of E-selectin in vascular injury with a flow chamber model and a rat model of carotid artery injury.

Methods and Results— We established a rat aortic endothelial cell (RAEC) culture system from the aortas of adult male rats. When rat myelomonocytes were suspended in a flow chamber, rolling and adhesion to lipopolysaccharide (LPS)-stimulated RAECs were observed. Cell rolling and adhesion were greatly reduced by addition of anti–E-selectin monoclonal antibody (mAb). We then induced balloon injury in the left carotid arteries of rats. E-selectin expression was enhanced in endothelial cells at adventitial small vessels 7 days after injury. Rats with balloon injury were injected intraperitoneally with anti–E-selectin mAb for 8 days. Inflammatory cell infiltration was reduced by anti–E-selectin mAb treatment at the adventitia at 7 days after injury. This reduction was associated with attenuation of intimal hyperplasia in the rats treated with the mAb.

Conclusions— These data suggest that E-selectin regulates adventitial inflammation through leukocyte adhesion and contributes to the process of intimal hyperplasia after balloon injury. (***Arterioscler Thromb Vasc Biol.* 2004; 24:2063-2068.**)

Key Words: adhesion molecules ■ adventitial inflammation ■ angioplasty ■ rat aortic endothelial cell ■ restenosis

Restenosis after percutaneous catheter intervention remains a serious clinical problem despite the development of new catheterization devices.[1–5] Neointima formation is caused by vascular smooth muscle cell proliferation. Various factors are involved in this process.[3–5] Among them, cell adhesion molecules are essential for the development of atherosclerosis.[6–8] A number of soluble factors are expressed by endothelial cells and recruited leukocytes.[7,9] P-selectin is one such cell adhesion molecule and is an established indicator of chronic and acute atherosclerotic events.[10–13] Elevated plasma levels of soluble P-selectin (sP-selectin) are associated with increased vascular injury in acute and chronic coronary artery disease (CAD).[12] We reported previously that anti–P-selectin monoclonal antibody (mAb) attenuates inflammatory responses and inhibits neointima formation in association with platelet accumulation after balloon injury of the carotid artery in rats.[13]

E-selectin assists in the rolling of leukocytes on activated endothelial cells and is expressed on the endothelium of atherosclerotic lesions.[7,9] Several studies have shown elevated plasma levels of soluble E-selectin (sE-selectin) in CAD. In one study, sE-selectin levels did not differ significantly between CAD patients and control subjects,[14] whereas other studies indicated that sE-selectin levels increased after angioplasty.[15,16] Examination of expression of cell adhesion molecule mRNAs in atherectomy specimens from patients with CAD revealed that expression of E-selectin mRNA was increased in restenosed coronary arteries in comparison with de novo lesions.[17] In peripheral arteries, vessel patency after angioplasty is associated with low levels of sE-selectin.[18] Despite these clinical findings, the role of E-selectin in acute vascular injury has not been investigated in animals. It is not known if blockade of E-selectin activity can attenuate intimal hyperplasia after vascular injury.

Thus, in the present study, we developed a new anti-rat E-selectin mAb and evaluated roles of E-selectin in the neointimal formation. We used an in vivo rat carotid artery balloon injury model and an in vitro flow chamber leukocyte

Original received January 16, 2004; final version accepted September 4, 2004.

From the Department of Cardiovascular Medicine (R.G., J.S., H.K., T.K., M.I.), Tokyo Medical and Dental University, Tokyo, Japan; Pharmaceutical Frontier Research Laboratories (S.S.), JT Inc, Yokohama, Japan; and the Department of Medical Biochemistry (M.Y.), Tokyo Medical and Dental University, Tokyo, Japan.

Correspondence to Mitsuaki Isobe, MD, Department of Cardiovascular Medicine, Tokyo Medical and Dental University, 1-5-45 Yushima, Bunkyo-ku, Tokyo 113-8519, Japan. E-mail isobemi.cvm@tmd.ac.jp

Arterioscler Thromb Vasc Biol. is available at http://www.atvbaha.org

DOI: 10.1161/01.ATV.0000145942.31404.20

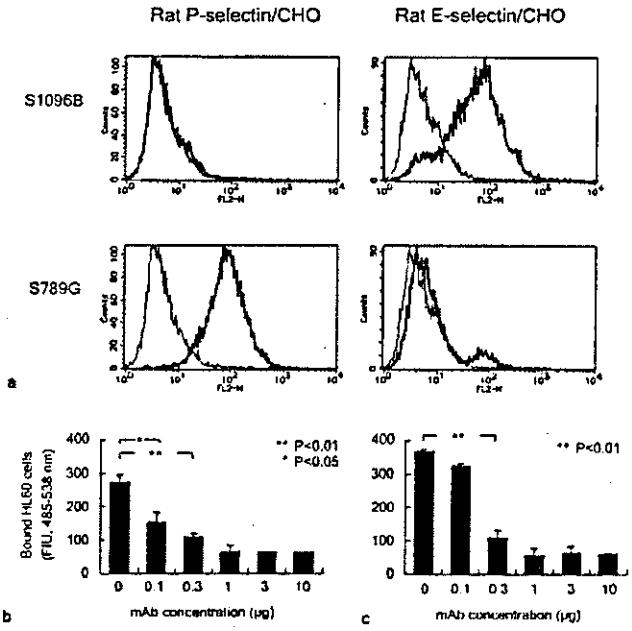

Figure 1. Characterization of mAb S1096B against E-selectin and mAb S789G against P-selectin. a, Binding specificity of S1096B (upper panel) and S789G (lower panel). Rat P-selectin–expressing CHO cells and rat E-selectin–expressing CHO cells were stained with mAbs (bold lines) or isotype control antibodies (thin lines). b, S1096B inhibited the binding of HL-60 cells to rat E-selectin–expressing CHO cells in a concentration-dependent manner. c, S789G inhibited the binding of HL-60 cells to rat P-selectin–expressing CHO cells in a concentration-dependent manner. Data are expressed as mean±SEM. FIU indicates fluorescence intensity unit; CHO, Chinese hamster ovary; mAb, monoclonal antibody.

adhesion model to test our hypothesis that expression of E-selectin can be a target for therapeutic intervention to reduce restenosis after angioplasty.

Methods

Animals

All animals were obtained from Japan SLC, Inc (Shizuoka, Japan) and were housed and handled as approved by the Institutional Animal Use and Care Committee of Tokyo Medical and Dental University. All experiments were conducted in conformity with the *Institutional Guidelines of Tokyo Medical and Dental University.*

Preparation of Anti-Rat E-Selectin MAb

Anti-rat E-selectin mAbs were generated by immunizing female BALB/c mice by footpad injection of 2 to 5×10^6 rat E-selectin–expressing Chinese hamster ovary (E-CHO). Popliteal lymph node cells were fused to mouse myeloma cells from the Japanese Collection of Research Bioresources (JCRB0113) with PEG4000 (Life Technologies, Inc, Grand Island, NY), and supernatants from the hybridomas were screened for the ability to bind to E-CHO cells. Cell binding assay was performed as described. The adhesion-blocking mAb was named S1096B. Anti-rat P-selectin mAb (S789G) was generated as previously described.[13,19] Specificities of these mAbs were confirmed by flow cytometry (Figure 1a). Flow cytometry was performed on a fluorescence-activated cell sorter Calibur (BD Bioscience) with these mAbs coupled to fluorescein isothiocyanate.

In Vitro Cell Binding Assay (Static)

E-CHO cells were plated at a concentration of 2×10^5 cells per well in 24-well multiplates and cultured overnight at 37°C under 5% CO_2. E-CHO monolayers were washed with phosphate-buffered saline and incubated with anti–E-selectin mAb at various concentrations (0.1, 0.3, 1, 3, 10 μg/mL) for 30 minutes at 4°C. Cultured HL-60 cells were suspended at a concentration of 1×10^7 cells/mL in RPMI1640 (Sigma, St. Louis, Mo) containing 10% fetal bovine serum (FBS) (Sigma). 3′-O-acetyl-2′,7′-bis (carboxyl-ethyl)-carboxyfluorescein diacetoxymethyl ester (BCECF-AM) was added to the cell suspension to a final concentration of 3 μmol/L. The cell suspension was incubated at 37°C for 30 minutes, and labeled cells were resuspended at a concentration of 2.5×10^5 cells/mL in RPMI1640 containing 1% FBS. Cell suspensions were plated at 200 μL/well, incubated for 30 minutes at 4°C, centrifuged at 120 rpm, and washed with phosphate-buffered saline containing 1% FBS. The attached cells were lysed with 1% Triton X-100 (Sigma). The fluorescence intensity unit of the cell lysates was measured with an excitation wavelength of 485 nm and an emission wavelength of 538 nm.

Rat Aortic Endothelial Cell Culture

Three male Sprague–Dawley rats weighing 300 to 400 grams were killed by an overdose injection of pentobarbital sodium. The thoracic aorta was removed immediately and washed with RPMI1640 containing 100 U/mL penicillin and 100 μg/mL streptomycin (Life Technologies, Inc). The aorta was filled with 1000 U/mL dispase (Godo Shusei, Tokyo, Japan) and 1% collagenase (Wako Pure Chemical Industries, Osaka, Japan) and incubated for 30 minutes at 37°C. The solution was then collected and centrifuged for 5 minutes at 1500 rpm. The supernatant was removed, and the cells were resuspended in RPMI1640 containing 10% FBS with 100 U/mL penicillin and 100 μg/mL streptomycin and 1 μg/mL amphotericin B (Sigma) and cultured on a rat collagen-I–coated dish (BD Biosciences). Rat aorta endothelial cells (RAECs) were identified by their characteristic cobblestone appearance, and identification was confirmed by the uptake of acetylated low-density lipoprotein labeled with 1,1′-dioctadecyl-1 to 3,3,3′,3′-tetramethylindocarbocyanine perchlorate (DiI-Ac-LDL; Biomedical Technologies, Inc., Stoughton, Mass).[20] RAECs at passages 5 through 7 were used for experiments.

Dynamic Flow Assay

Two hundred microliters of RAEC suspension was put on a rat collagen-I–coated coverslip (BD Biosciences) and placed over a 6-well plate at a seeding density of 3×10^5 cells/mL. Three days later, RAECs were stimulated by 1 μg/mL lipopolysaccharide (LPS) (from *Escherichia coli* serotype O127:B8; Sigma) for 4 hours. Cells were washed twice with RPMI1640 containing 1% FBS and incubated with or without antibody (10 μg/mL) S1096B or MOPC-21 (non-immunized mouse IgG1; PharMingen, San Diego, Calif). The flow chamber was constructed as described previously.[21] A plastic heating plate (Tokai Hit Co) was mounted on the stage of an inverted microscope (IX50; Olympus) to maintain the temperature of the chamber at 37°C. The coverslip was attached to the chamber placed on the microscope stage. The system was then filled with 1×10^6 cells/mL of rat myelomonocytic cell (c-WRT-7-LR, Health Science Research Resources Bank, JCRB0168)[22,23] suspended in adhesion media (Dulbecco modified phosphate-buffered saline + 0.9 mmol/L $CaCl_2$ + 0.2% human albumin). This suspension was drawn off at controlled flow rates with a syringe pump (Model 44; Harvard Apparatus) connected to the outlet flow chamber to generate calculated wall shear stresses of 1.0 dyne/cm^2 for 10 minutes. The perfusion period was videotaped with a digital video recorder containing a time generator. The captured images were transferred to a PC computer for image analysis to determine the number of rolling and adherent c-WRT-7-LR cells in 5 to 10 randomly selected 200× microscopic fields for each experiment. Cells were considered adherent after 10 seconds of stable contact with the monolayer. Rolling leukocytes were easily recognized because their velocities were much slower (up to 80 μm/s) than those of free-flowing cells.

Vascular Injury Model

Male Sprague–Dawley rats were anesthetized by intraperitoneal administration of pentobarbital sodium (50 mg/kg). The rat carotid

arteries were dilated and denuded of endothelium with a 2-French Fogarty balloon embolectomy catheter (Baxter Health Care) introduced into the left common carotid artery through the external carotid artery.[24,25] The catheter was retracted 3 times. After the catheter was removed, the external carotid artery was ligated.

MAb Treatment Study

Rats were assigned randomly to 1 of 4 treatment groups: MOPC-21 (nonimmunized IgG) treatment (group C), S1096B (anti–E-selectin mAb) treatment (group E), S789G (anti–P-selectin mAb) treatment (group P), and both S1096B and S789G treatment (group E+P). MAbs were administered intraperitoneally to rats at a dosage of 4 mg/kg 30 minutes before arterial injury and once daily for 7 consecutive days after injury as previously reported.[13] Carotid arteries were harvested 14 days (n=8, each group) and 56 days (n=8, each group) after balloon injury.

Histology and Morphometry

Treated rats were euthanized by overdose injection of pentobarbital, and the injured carotid artery was then perfusion-fixed at 100 mm Hg and embedded in paraffin. Each artery was stained with van Gieson elastin stain and subjected to blinded morphometric examination under a video microscope (HC-300I; Nikon) equipped with a computerized digital image analysis system (SCION Image, public domain software). The areas of the external elastic lamina (EEL), the internal elastic lamina (IEL), and the lumen were measured. Medial and neointimal areas were calculated as follows: medial area=EEL area − IEL area; neointimal area=IEL area − lumen area; neointima/media (I/M) ratio=neointimal area/medial area. The circumferences (lengths) of the EEL and IEL were also measured to determine vascular shrinking.

Immunohistochemical Study

Harvested carotid arteries were immediately embedded in optimal cutting temperature compound and frozen at −20°C. Immunohistochemical analysis was performed on the frozen sections. A Vectastain Elite ABC kit (Vector Laboratories) was used on the sections with S1096B (anti–E-selectin), S789G (anti–P-selectin), anti-CD31 antibody (PharMingen), anti-CD45 antibody (PharMingen), anti–ED-1 antibody (Cosmo Bio, Tokyo, Japan), and MOPC-21 (nonimmunized IgG) as primary antibodies. Sections were incubated with diaminobenzidine (Vector Laboratories) at 100 mg/mL for 5 minutes, counterstained with hematoxylin, and then mounted permanently with coverslips.

Statistical Analysis

All data are presented as mean±SEM. Experimental groups were compared with 1-way analysis of variance and a post hoc test (Fisher protected least significant difference) for multiple comparisons. Values derived from the dynamic flow assay were compared by Mann–Whitney U test. $P<0.05$ were considered statistically significant.

Results

Characterization of Anti–E-Selectin Monoclonal Antibody (S1096B)

S1096B is a mouse IgG1 antibody. The specificity of this anti–E-selectin mAb was confirmed by flow cytometry by binding to E-CHO cells. S1096B bound to E-CHO cells but not to P-selectin–expressing CHO cells (P-CHO). S789G bound to P-CHO cells, but not to E-CHO cells (Figure 1a). HL-60 cells adhered to E-CHO cells untreated with antibody. S1096B blocked adhesion of HL-60 cells to E-CHO cells in a concentration-dependent manner (Figure 1b). S789G blocked adhesion of HL-60 cells to P-CHO cells in a concentration-dependent manner (Figure 1c).

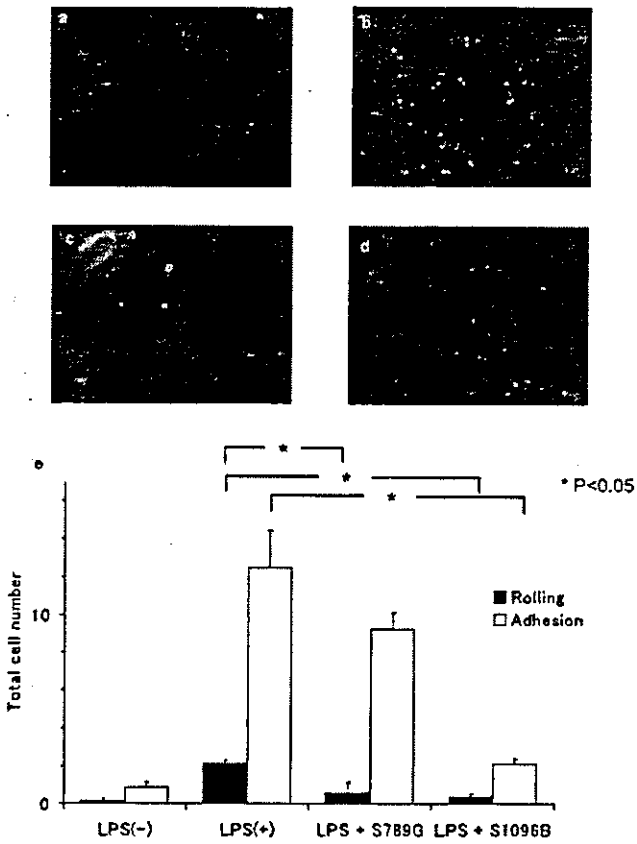

Figure 2. Effect of mAb S1096B against E-selectin and mAb S789G against P-selectin under physiological flow conditions. Rat myelomonocytic cells (c-WRT-7-LR) were suspended in a flow chamber with a rat aorta endothelial cell (RAEC)-cultured coverslip. a, The cells did not adhere to unstimulated RAECs. b, The cells did adhere to RAECs stimulated with LPS. c, S1096B inhibited this adhesion. d, S789G less inhibited this adhesion. e, Number of c-WRT-7-LR cells adhered to stimulated RAECs. The number of rolling and adhering cells was reduced by treatment with S1096B. Addition of S789G reduced the number of rolling cells but did not reduce the number of adherent cells. Data are expressed as mean±SEM. Bar=10 μm.

S1096B Blocks E-Selectin–Dependent Rolling and Adhesion Under Flow Conditions

Under flow conditions, c-WRT-7-LR cells did not roll or adhere to unstimulated RAECs (0.86±0.26 cells/field) (Figure 2a). When RAECs were stimulated with LPS, adhesion of c-WRT-7-LR cells was detected (data not shown). This adhesion was not changed after incubation with MOPC-21 (nonimmune IgG) (12.50±1.97 cells/field) (Figure 2b and 2e) but was reduced significantly by addition of S1096B (2.13±0.30 cells/field; $P<0.01$) (Figure 2c and 2e). Addition of S789G did not significantly reduce adhesion (Figure 2d and 2e). Rolling of c-WRT-7-LR cells was observed after RAECs stimulated with LPS were incubated with MOPC-21 (2.13±0.72 cells/field). Rolling was significantly reduced by treatment with S1096B or S789G (0.38±0.18 cells/field, 0.60±0.51 cells/field; $P<0.05$) (Figure 2e).

Expression of E-Selectin After Vascular Injury In Vivo

Representative photomicrographs of arteries harvested and sectioned 7 days after balloon injury and stained with

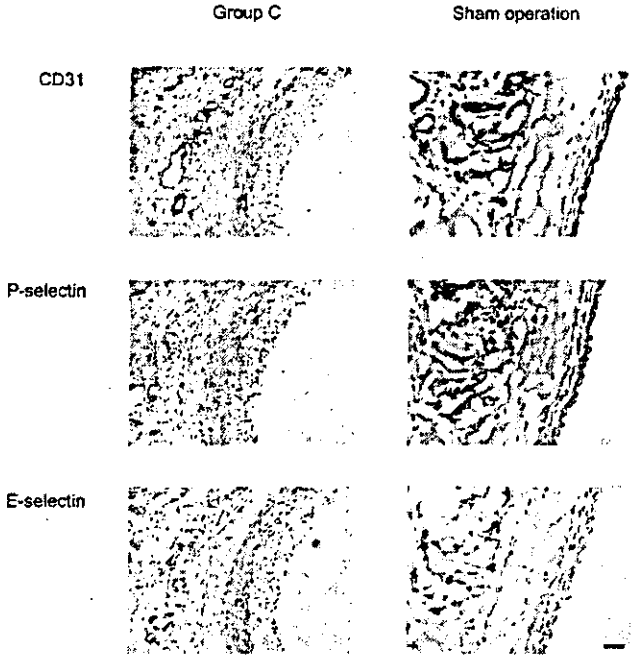

Figure 3. Representative frozen sections of rat carotid arteries at 7 days after balloon injury treated with control IgG (group C) and those of uninjured artery (sham operation). Immunostaining with anti-CD31 antibody, anti–P-selectin antibody, and anti–E-selectin antibody. In group C, E-selectin and P-selectin staining was enhanced in adventitial endothelial cells in the *vasa vasorum*. In the sham operation group, faint staining of both selectins was noted. Bar=10 μm.

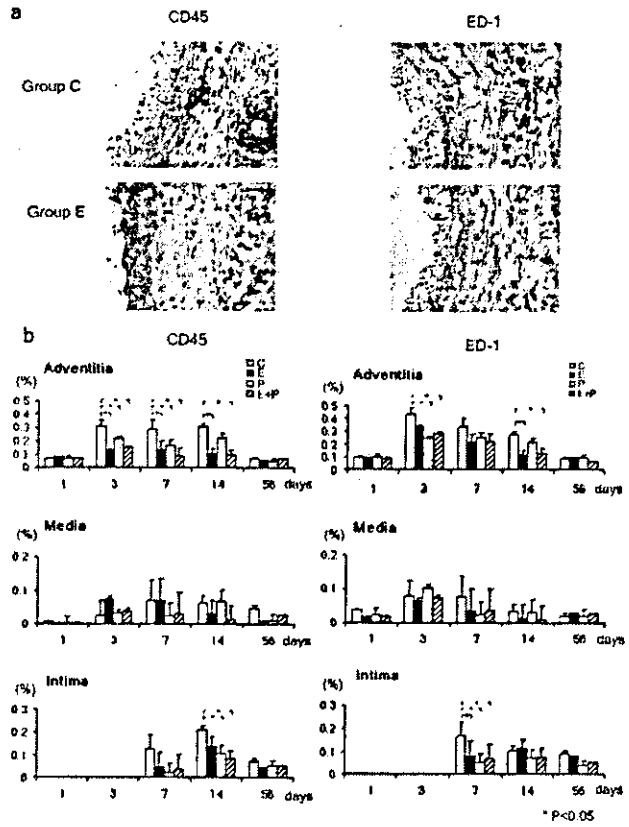

Figure 4. a, Representative frozen sections of rat carotid arteries at 7 days after balloon injury treated with control IgG (group C) and anti–E-selectin mAb (group E). b, Analysis of CD45-positive and ED-1–positive cells in the 4 groups over time. Rats were treated with control IgG (group C), anti–E-selectin mAb (group E), anti–P-selectin mAb (group P), or anti–E-selectin and anti–P-selectin mAbs (group E+P). Left, Percentages of CD45-positive cells in the adventitial (upper), medial (middle), and intimal (lower) layers over time. Right, Percentages of ED-1–positive cells in the adventitial (upper), medial (middle), and intimal (lower) layers over time. Data are expressed as mean±SEM.

antibody to E-selectin or P-selectin are shown in Figure 3. Positive staining was not observed in sections stained with control IgG (data not shown). We used anti-CD31 antibody to visualize endothelial cells. Most CD31-positive cells were present in the adventitia, indicating that the injured lumina had not yet re-endothelialized at 7 days after injury. E-selectin and P-selectin staining of adventitial endothelial cells was increased. In the sham operation group, faint staining of both selectins was detected.

S1096B Blocks E-Selectin–Dependent Leukocyte Accumulation

We examined the effect of S1096B on leukocyte accumulation after vascular injury by immunohistochemistry. We used anti-CD45 antibody to detect leukocytes and anti–ED-1 antibody to detect macrophages (Figure 4a) and analyzed percentages of CD45-positive and ED-1–positive cells over time (Figure 4b). At days 1 and 3 after injury, the intima and media could not be clearly differentiated. In the early period after vascular injury, CD45-positive and ED-1–positive cells accumulated predominantly in the adventitia. With the progression of intimal hyperplasia, these cells transmigrated into the intima. The accumulation of CD45-positive and ED-1–positive cells in the adventitia was inhibited by treatment with S1096B.

Inhibition of E-Selectin–Dependent Adhesion Attenuates Injury-Induced Intimal Hyperplasia and Vascular Remodeling

There was no significant difference in body weight between groups of rats. Morphometric analysis is shown in Figure 5a.

The I/M ratio of group E was significantly less than that of group C at 8 weeks after injury (1.49±0.20 versus 2.07±0.14; $P<0.05$). The ratios at 2 weeks after injury did not differ statistically (1.40±0.11 versus 1.62±0.15) (Figure 5a, left). The I/M ratio of group P and that of group E+P were significantly lower than that of group C at 2 weeks after injury (1.16±0.17 and 1.10±0.09, respectively, versus 1.62±0.15, $P<0.05$). The I/M ratio of group P was not different from that of group E+P at 2 and 8 weeks after injury. Thus, a synergistic effect of dual blockade of E-selectin and P-selectin was not identified. The neointimal areas in group E and group P were reduced compared with that in group C at 8 weeks after injury. The medial area in each of the 4 groups did not differ significantly at 8 weeks after injury (Figure 5a, right).

Morphometric analysis showed that IEL and EEL lengths are significantly greater in the mAb treatment groups (group E, group P, and group E+P) than group C at 8 weeks after injury indicating suppression of negative remodeling (Figure 5b). A synergistic effect of dual blockade of E-selectin and P-selectin was not identified in this analysis. Representative

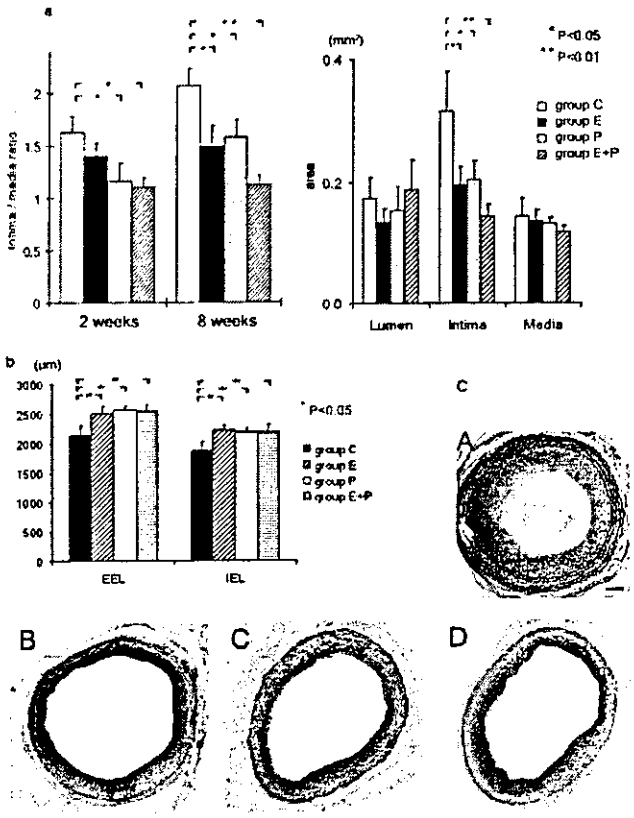

Figure 5. a, Morphological analysis of rat carotid arteries after balloon injury. Rats were treated with control IgG (group C), anti–E-selectin mAb (group E), anti–P-selectin mAb (group P), or anti–E-selectin and anti–P-selectin mAbs (group E+P). Left panel shows analysis of intima/media (I/M) ratio at 2 weeks and 8 weeks after injury. Right panel shows the neointimal area and the medial area in each group at 8 weeks after injury. b, Morphometric analysis of internal elastic lamina circumference length (IEL) and external elastic lamina circumference length (EEL) at 8 weeks after injury. These parameters in group E, group P, or group E+P are significantly greater than that in group C. c, Photomicrographs of representative cross-sections of rat left common carotid arteries in each group at 8 weeks after injury. A indicates group C; B, group E; C, group P; D, group E+P. Data are expressed as mean±SEM. Bar=100 μm; van Gieson elastin stain.

images of left common carotid artery sections in the 4 groups at 8 weeks after injury are shown in Figure 5c.

Discussion

In the present study, we found that anti–E-selectin mAb S1096B blocked rolling and adhesion of myelomonocytes on aortic endothelial cells in an in vitro flow chamber model. Our in vivo study showed that anti–E-selectin mAb attenuated intimal hyperplasia after balloon injury, with significantly reduced infiltration of leukocytes in the adventitia.

E-selectin mediates rolling of leukocytes at the site of inflammation,[7,9] and expression of E-selectin is limited to endothelial cells in inflamed tissue.[9] E-selectin cannot play a role in the earliest phases of acute inflammation because de novo gene transcription is necessary for expression.[9] Our immunohistochemical studies showed that normal vessel walls do not express E-selectin. Similarly, myelomonocytes did not adhere to unstimulated RAECs. We found that injured lumina had not re-endothelialized at 7 days after balloon injury and that E-selectin was not expressed on the luminal side but was expressed on endothelial cells in the adventitia. Most inflammatory cells were identified in the adventitia, particularly in the *vasa vasorum*, and anti–E-selectin mAb reduced the infiltration of inflammatory cells in this region at this stage. Thus, E-selectin plays a role in leukocyte accumulation in the adventitia in our model of vascular injury.

Mechanical injury of arteries leads to the infiltration of inflammatory cells;[24] release of chemokines,[26] cytokines,[27] and other chemical mediators;[28] transmigration of monocytes and macrophages;[6] and proliferation of vascular smooth muscle cells.[6,7,24,26,27] Our findings indicate that suppression of inflammatory cell infiltration into the adventitia by anti–E-selectin mAb is associated with reduced intimal hyperplasia after balloon injury. Thus, inflammation in the adventitia could be an important factor in the development of intimal hyperplasia and vascular shrinkage.

The mechanism of adventitial inflammation in intimal hyperplasia is unknown. The intensity of the adventitial inflammatory response correlates with the severity of atherosclerosis and restenosis after balloon angioplasty.[29,30] Although we did not determine the role of E-selectin in these processes in the present study, there are several possible mechanisms. For example, inflammatory cells that infiltrate in response to enhanced E-selectin expression in the adventitia may release a variety of chemical mediators, including cytokines, chemokines, and growth factors, which promote transmigration and proliferation of vascular smooth muscle cells in the media and lead to hyperplasia of the intima. In addition, our data show improvement of vascular shrinkage after mAb treatment, indicating that inflammation of the adventitia leads to negative remodeling of the injured vessels. This remodeling could be reduced by anti-selectin treatment.

Our previous study showed that an anti–P-selectin mAb reduces the accumulation of leukocytes in the adventitia and neointima and prevents neointimal formation at 2 weeks after balloon injury.[13] Similar results were obtained in the present study. According to our previous study,[13] expression of P-selectin on platelets is important for suppression of inflammation and for reduction of intimal formation. In the present study, anti–E-selectin mAb significantly attenuated intimal hyperplasia at 8 weeks after injury. However, it did not attenuate intimal hyperplasia at 2 weeks after injury. Unlike E-selectin, P-selectin expression by endothelial cells and platelets does not require de novo gene transcription. Therefore, P-selectin responds immediately to acute inflammation that is caused by arterial injury. These differences between the 2 selectins may account for their different roles in intimal thickening. We suggest that adventitial inflammation mediates late-stage intimal hyperplasia via expression of E-selectin. This is supported by our analysis of inflammatory cell infiltration overtime, as shown in Figure 4. Cell infiltration in the adventitia was observed initially at 3 days after induction of injury. This was followed by inflammation in the intima at 7 to 14 days after injury and by intimal hyperplasia at later stages. Anti–E-selectin mAb suppressed early-stage adventitial infiltration. Therefore, it is reasonable to speculate that inhibition of adventitial inflammation by blockade of

E-selectin–dependent cell adhesion leads to the attenuation of intimal hyperplasia observed at 8 weeks after injury.

Because P-selectin and E-selectin play different roles in the recruitment of leukocytes into the site of inflammation, a synergistic action of dual blockade of the 2 selectins was expected. However, we did not observe such synergism in the present study. Tendencies toward decreased I/M ratios and intimal areas but without statistical significance were detected. Also, the IEL and EEL lengths of group P and group E were not different from those of group E+P at 8 weeks after injury. Possible synergism of these selectins will be studied in future experiments.

In conclusion, these data suggest that E-selectin controls adventitial inflammation through leukocyte adhesion and contributes to the process of intimal hyperplasia in the late stage after balloon injury. Blockade of E-selectin may be a new strategy to control restenosis after coronary balloon angioplasty.

Acknowledgments

We thank Professor Ikuo Morita for advice and help with endothelial cell cultures. We thank Noriko Tamura and Megumi Hiraoka for excellent technical assistance. This investigation was supported by a grant-in-aid from the Japanese Ministry of Science, Education, and Culture.

References

1. Landou C, Lange RA, Hillis LD. Percutaneous transluminal coronary angioplasty. *N Engl J Med.* 1994;330:981–993.
2. Currier JW, Faxon DP. Restenosis after percutaneous transluminal coronary angioplasty: have we been aiming at the wrong target? *J Am Coll Cardiol.* 1995;25:516–520.
3. Bauters C, Meurice T, Hamon M, McFadden E, Lablanche JM, Bertrand ME. Mechanisms and prevention of restenosis: from experimental models to clinical practice. *Cardiovasc Res.* 1996;31:835–846.
4. Berk BC, Harris K. Restenosis after percutaneous transluminal coronary angioplasty: new therapeutic insights from pathogenic mechanisms. *Adv Intern Med.* 1995;40:445–501.
5. Lefkowitz R, Willerson J. Prospects for cardiovascular research. *JAMA.* 2001;285:581–587.
6. Cybulsky MI, Gimbrone MA Jr. Endothelial expression of a mononuclear leukocyte adhesion molecule during atherogenesis. *Science.* 1991;251:788–791.
7. Price DT, Loscalzo J. Cellular adhesion molecules and atherogenesis. *Am J Med.* 1999;107:85–97.
8. Kawamura A, Miura S, Murayama T, Iwata A, Zhang B, Nishikawa H, Tsuchiya Y, Matsuo K, Tsuji E, Saku K. Increased expression of monocytes CD11c and intracellular adhesion molecule-1 in patients with initial atherosclerotic coronary stenosis. *Circ J.* 2004;68:6–10.
9. Carlos T, Harlan J. Leukocyte-endothelial adhesion molecules. *Blood.* 1994;84:2068–2101.
10. Mickelson JK, Lakkis NM, Villarreal-Levy G, Hughes BJ, Smith CW. Leukocyte activation with platelet adhesion after coronary angioplasty: a mechanism for recurrent disease? *J Am Coll Cardiol.* 1996;28:345–353.
11. Ishiwata S, Tukada T, Nakanishi S, Nishiyama S, Seki A. Postangioplasty restenosis: platelet activation and the coagulation fibrinolysis system as possible factors in the pathogenesis of restenosis. *Am Heart J.* 1997;133:387–392.
12. Hollander JE, Muttreja MR, Dalesandro MR, Shofer FS. Risk stratification of emergency department patients with acute coronary syndromes using P-selectin. *J Am Coll Cardiol.* 1999;34:95–105.
13. Hayashi S, Watanabe N, Nakazawa K, Suzuki J, Tsushima K, Tamatani T, Sakamoto S, Isobe M. Roles of P-selectin in inflammation, neointimal formation, and vascular remodeling in balloon-injured rat carotid arteries. *Circulation.* 2000;102:1710–1717.
14. Porsch-Oezcueruemez M, Kunz D, Kloer HU, Luley C. Evaluation of serum levels of solubilized adhesion molecules and cytokine receptors in coronary heart disease. *J Am Coll Cardiol.* 1999;34:1995–2001.
15. Kurz RW, Graf B, Gremmel F, Wurnig C, Stockenhuber F. Increased serum concentrations of adhesion molecules after coronary angioplasty. *Clin Sci.* 1994;87:627–633.
16. Schulze PC, Kluge E, Schuler G, Lauer B. Periprocedural kinetics in serum levels of cytokines and adhesion molecules in elective PTCA and stent implantation: impact on restenosis. *Arterioscler Thromb Vasc Biol.* 2002;22:2105–2107.
17. Ishibashi T, Kijima M, Yokoyama K, Shindo J, Nagata K, Hirosaka A, Techigawara M, Abe Y, Sato E, Yamaguchi N, Watanabe N, Saito T, Maehara K, Ohmoto Y, Maruyama Y. Expression of cytokine and adhesion molecule mRNA in atherectomy specimens from patients with coronary artery disease. *Jpn Circ J.* 1999;63:249–254.
18. Belch JJ, Shaw JW, Kirk G, McLaren M, Robb R, Maple C, Morse P. The white blood cell adhesion molecule E-selectin predicts restenosis in patients with intermittent claudication undergoing percutaneous transluminal angioplasty. *Circulation.* 1997;95:2027–2031.
19. Katayama T, Ikeda Y, Handa M, Tamatani T, Sakamoto S, Ito M, Ishimura Y, Suematsu M. Immunoneutralization of glycoprotein Ib α attenuates endotoxin-induced interactions of platelets and leukocytes with rat venular endothelium in vivo. *Circ Res.* 2000;86:1031–1037.
20. Voyta JC, Via DP, Butterfield CE, Zetter BR. Identification and isolation of endothelial cells based on their increased uptake of acetylated-low density lipoprotein. *J Cell Biol.* 1984;99:2034–2040.
21. Yoshida M, Sawada T, Ishii H, Gerszten RE, Rosenzweig A, Gimbrone MA Jr., Yasukochi Y, Numano F. HMG-CoA reductase inhibitor modulates monocyte-endothelial cell interaction under physiological flow conditions in vitro: involvement of Rho GTPase-dependent mechanism. *Arterioscler Thromb Vasc Biol.* 2001;21:1165–1171.
22. Fujii T, Takeichi N, Kasai M, Moriuchi T, Kobayashi H. Establishment and characterization of a differentiating myeloid cell line obtained from a rat myelomonocytic leukemia. *Cancer Res.* 1983;43:1875–1879.
23. Fujii Y, Yuki N, Takeichi N, Kobayashi H, Miyazaki T. Differentiation therapy of a myelomonocytic leukemia (c-WRT-7) in rats by injection of lipopolysaccharide and daunomycin. *Cancer Res.* 1987;47:1668–1673.
24. Clowes AW, Reidy MA, Clowes MM. Kinetics of cellular proliferation after arterial injury. I. Smooth muscle growth in the absence of endothelium. *Lab Invest.* 1983;49:327–333.
25. Reidy M, Clowes A, Schwartz S. Endothelial regeneration. V. Inhibition of endothelial regrowth in arteries of rat and rabbit. *Lab Invest.* 1983;49:569–575.
26. Welt FG, Tso C, Edelman ER, Kjelsberg MA, Paolini JF, Seifert P, Rogers C. Leukocyte recruitment and expression of chemokines following different forms of vascular injury. *Vasc Med.* 2003;8:1–7.
27. Wainwright CL, Miller AM, Wadsworth RM. Inflammation as a key event in the development of neointima following vascular balloon injury. *Clin Exp Pharmacol Physiol.* 2001;28:891–895.
28. Kennedy S, McPhaden AR, Wadsworth RM, Wainwright CL. Correlation of leukocyte adhesiveness, adhesion molecule expression and leukocyte-induced contraction following balloon angioplasty. *Br J Pharmacol.* 2000;130:95–103.
29. Wilcox JN, Scott NA. Potential role of the adventitia in arthritis and atherosclerosis. *Int J Cardiol.* 1996;54:S21–S35.
30. Wilcox JN, Okamoto EI, Nakahara KI, Vinten-Johansen J. Perivascular responses after angioplasty which may contribute to postangioplasty Restenosis: a role for circulating myofibroblast precursors? *Ann N Y Acad Sci.* 2001;947:68–92.

Pitavastatin Inhibits Remnant Lipoprotein-Induced Macrophage Foam Cell Formation Through ApoB48 Receptor–Dependent Mechanism

Akio Kawakami, Mariko Tani, Tsuyoshi Chiba, Katsumasa Yui, Shohei Shinozaki, Katsuyuki Nakajima, Akira Tanaka, Kentaro Shimokado, Masayuki Yoshida

Objective—Atherogenic remnant lipoproteins (RLPs) are known to induce foam cell formation in macrophages in vitro and in vivo. We examined the involvement of apoB48 receptor (apoB48R), a novel receptor for RLPs, in that process in vitro and its potential regulation by pitavastatin.

Methods and Results—THP-1 macrophages were incubated in the presence of RLPs (20 mg cholesterol/dL, 24 hours) isolated from hypertriglyceridemic subjects. RLPs significantly increased intracellular cholesterol ester (CE) and triglyceride (TG) contents (4.8-fold and 5.8-fold, respectively) in the macrophages. Transfection of THP-1 macrophages with short interfering RNA (siRNA) against apoB48R significantly inhibited RLP-induced TG accumulation by 44%. When THP-1 macrophages were pretreated with pitavastatin (5 μmol/L, 24 hours), the expression of apoB48R was significantly decreased and RLP-induced TG accumulation was reduced by 56%. ApoB48R siRNA also inhibited TG accumulation in THP-1 macrophage induced by β–very-low-density lipoprotein derived from apoE−/− mice by 58%, supporting the notion that apoB48R recognizes and takes-up RLPs in an apoE-independent manner.

Conclusions—RLPs induce macrophage foam cell formation via apoB48R. Pitavastatin inhibits RLP-induced macrophage foam cell formation. The underlying mechanism involves, at least in part, inhibition of apoB48R-dependent mechanism. Our findings indicate a potential role of apoB48R in atherosclerosis. (***Arterioscler Thromb Vasc Biol.*** **2005; 25:424-429.)**

Key Words: remnant lipoproteins ■ foam cell formation ■ apoB48 receptor ■ statin ■ atherosclerosis

Clinical studies have revealed that remnant lipoproteins (RLPs), which are produced by hydrolysis of chylomicrons (CMs) and very-low-density lipoproteins (VLDL), are closely related to atherosclerosis, independent of high-density lipoprotein and low-density lipoprotein (LDL).[1,2] There is also increasing evidence that RLPs play a causative role in atherogenesis, and we recently reported that they induced monocyte-endothelial interaction and vascular smooth muscle cell proliferation.[3,4] However, the effect(s) of RLPs on cellular mechanism(s) during atherogenesis have not been fully elucidated.

Atherogenesis involves the appearance of lipid-loaded foam cells derived from macrophages in the arterial intima. RLPs from hypertriglyceridemic VLDL and CMs cause rapid lipid accumulation, and induce foam cell formation in macrophages, whereas normal VLDL and LDL do not.[5] Thus, inhibition of macrophage foam cell formation induced by RLPs may contribute to the prevention of atherosclerosis. It has been reported that mechanisms independent of apolipoprotein (apo) E and LDL receptor family are involved in lipid accumulation in macrophages.[6] Recently, apoB48 receptor (apoB48R) was shown to be involved in the uptake of triglyceride-rich lipoproteins (TRLs) and contribute to atherogenesis,[7] although the role of apoB48R in this process remains unclear. Herein, we report for the first time to our knowledge the dominant role of apoB48R in RLP-induced foam cell formation by selective downregulation of apoB48R with short interfering RNA (siRNA).

Recently, 3-hydroxy-3-methylglutaryl (HMG)-coenzyme A (CoA) reductase inhibitor, or statin, has been suggested to have beneficial effects for the prevention of atherosclerosis, independent of its LDL cholesterol-lowering effect.[8] We found that statins reduced monocyte adhesion to endothelial cells via inhibition of Rho GTPase pathway.[3,9] In the present study, treatment with pitavastatin lowered RLP-induced macrophage foam cell via, at least in part, inhibition of the expression of apoB48R in THP-1 macrophages. Our results suggest that apoB48R pathway might be a novel therapeutic

Original received March 23, 2004; final version accepted November 4, 2004.

From the Departments of Geriatrics and Vascular Medicine (A.K., M.T., T.C., K.Y., S.S., K.S., M.Y.) and Medical Biochemistry (A.K., M.T., M.Y.), Graduate School of Medicine, Tokyo Medical and Dental University, Tokyo, Japan; Japan Immunoresearch Laboratories (K.N.), Takasaki, Japan; and the Department of Health and Nutrition (A.T.), College of Human Environmental Studies, Kanto-Gakuin University, Yokohama, Japan.

Correspondence to Masayuki Yoshida, MD, Department of Medical Biochemistry, Graduate School of Medicine, Tokyo Medical and Dental University, 1-5-45, Yushima, Bldg. D-809, Bunkyo-ku, Tokyo 1138519 Japan. E-mail masa.vasc@tmd.ac.jp

Arterioscler Thromb Vasc Biol. is available at http://www.atvbaha.org

DOI: 10.1161/01.ATV.0000152632.48937.2d

target for atherogenesis, particularly in hypertriglyceridemic patients. Further, pitavastatin may exert a beneficial effect on atherogenesis by suppressing this pathway.

Methods

Reagents and Cell Culture

Pitavastatin was kindly provided by Kowa Pharmaceutical Company, Tokyo, Japan. Phorbol-12-myristate-13-acetate (PMA), C3 exoenzyme, farnesyl-pyrophosphate (FPP), and geranylgeranyl-pyrophosphate (GGPP) were purchased from Wako. RPMI 1640, DMEM, and FBS were obtained from GIBCO BRL. Antibodies used in the present study were as follows: mouse anti-RhoA monoclonal antibody (Santa Cruz Biotechnology), rabbit anti-GAPDH antibody (Sigma), HRP-conjugated goat anti-mouse IgG, and HRP-conjugated goat anti-rabbit IgG (Cal-tag). Rabbit anti-human apoB48R antibody was a generous gift from Dr Sandra H. Gianturco and Dr William A. Bradley, The University of Alabama at Birmingham.

Human monocytic THP-1 cells were obtained from American Type Culture Collection and maintained in RPMI 1640 medium supplemented with 10% FCS, 100 U/mL penicillin, 100 mg/mL streptomycin, and 2 mmol/L L-glutamine in a humidified atmosphere of 5% CO_2 at 37°C. To obtain THP-1 macrophages, THP-1 cells were plated in 35-mm dishes (1×10^7 cells/dish) and incubated with PMA at a concentration of 200 nmol/L for 4 days. Human peripheral blood monocytes were isolated from healthy volunteers using Ficoll-Paque (Pharmacia Biotech) and a monocyte-negative isolation kit (Miltenyi Biotech). To examine cell viability, cells were stained with 4′, 6-Diamidino-2-phenylindole dihydrochloride (DAPI; 200 ng/mL) (Dojindo), and viable cells were counted at the required time point using a hemacytometer.

Lipoprotein Preparation

EDTA plasma was obtained from 24 patients with hypertriglyceridemia who showed an elevated RLP concentration (>7.5 mg cholesterol/dL) 4 hours after eating breakfast. They had no cardiovascular diseases or diabetes and had not taken cardiovascular medicine or antioxidants. The protocol of this study complied with the guidelines for the conduct of research involving human subjects by the Committee on Human Research at Tokyo Medical and Dental University. RLPs were isolated from plasma samples using an RLP-C Kit, as described previously,[10] then dialyzed overnight against 5 L of PBS containing 50 μmol/L EDTA (pH 7.4) and sterilized using a 0.22-μm filter unit (Millipore). The prepared RLPs were analyzed by SDS-PAGE in a 5% to 20% linear gradient gel (Funakoshi) and visualized with a silver stain reagent (Daiichi). Densitometry showed that apoB48 comprised only 5% to 7% of total apoB in RLPs, as we and others reported previously.[3,11] β-VLDL (density<1.006 g/mL) was isolated from freshly prepared plasma taken from apoE−/− mice (obtained from Jackson Laboratory, Bar Harbor, Me, and fed a normal diet) at 8 weeks of age by ultracentrifugation.

Oil Red O Staining

THP-1 macrophages were seeded into multi-well slides (Nunc) at a concentration of 1×10^6 cells per well. The cells were washed 3 times with phosphate-buffered saline, fixed with formaldehyde, and stained with oil red O. Lipid accumulation was observed under a microscope.

Cellular Lipid Analysis

To determine intracellular lipid contents, THP-1 macrophages were removed from the culture plates and washed twice with phosphate-buffered saline. Then, intracellular lipids were extracted using isopropanol/hexane. Cholesterol ester, triglyceride (TG), and protein mass were determined enzymatically.

Immunoblotting

Cells were disrupted in a lysis buffer and total cell lysates prepared. An equal amount of protein (10 μg) was subjected to SDS-PAGE, after which immunoblotting was performed using the indicated antibodies. Immunoreactive proteins were detected using an enhanced chemiluminescence advance (Amersham Pharmacia Biotech). For a RhoA translocation assay, cell lysates from the membranes and cytosol fractions were prepared as described previously.[9]

Transfection of siRNA Against ApoB48R

siRNA was designed to target the coding sequence of human apoB48R cDNA. The target sequences were directed to the single-strand region according to the predicted secondary RNA structure and sequences of the form $(AA/CA)N_{19}$ with GC contents of <70% were selected from this region.[12] Nineteen nucleotide RNAs followed by TT/TG were selected, then chemically synthesized and gel-purified. Sequences corresponding to the siRNA were nucleotides 1060 to 1079 for apoB48R coding region (GenBank accession number AF141332). Nonrelevant 19 RNAs were used to generate the control siRNA. Double-stranded siRNAs were generated and transfected into THP-1 macrophages, as described previously.[13] Transfection efficiency was evaluated using BLOCK-IT Fluorescent dsRNA (Invitrogen);[14] 64.3±13.8% of THP-1 macrophages were positive for fluorescein isothiocyanate 48 hours after transfection.

RhoA Pull-Down Assay

RhoA pull-down assay was performed using Rho activation kit (Upstate) following the manufacturer's protocol.[15]

Statistical Analysis

Results are presented as the mean±SD. Data were analyzed using analysis of variance (ANOVA), with a value of $P<0.05$ considered significant.

Results

RLPs Induce Foam Cell Formation in THP-1 Macrophages

We investigated whether RLPs could induce macrophage foam cell formation. First, THP-1 cells were incubated in the presence of PMA at a concentration of 200 nmol/L for 4 days for full differentiation. After the medium was replaced with fresh medium with or without RLPs, THP-1 cells were incubated for an additional 24 hours. Oil red O staining showed that treatment with RLPs induced foam cell formation in PMA-treated THP-1 macrophages (Figure 1). Intracellular TG and cholesterol ester contents in the cells were also significantly increased 24 hours after the addition of RLPs in a dose-dependent manner (Figure 1).

Expression of Remnant Receptors During Differentiation in THP-1 Macrophages

To elucidate the mechanism(s) by which RLPs induce macrophage foam cell formation, we examined the expression levels of representative remnant receptors and related proteins with immunoblotting.[16] During the differentiation process, immunoreactive LDL receptors nearly disappeared. In contrast, CD36, a scavenger receptor not present in THP-1 monocytes, appeared after PMA treatment, indicating that THP-1 monocytes differentiated into macrophages (Figure 2A). LDL receptor–related protein (LRP) was not detected throughout the differentiation process (data not shown). Interestingly, the expression level of apo48R, which is present in monocytes, remained unchanged throughout the

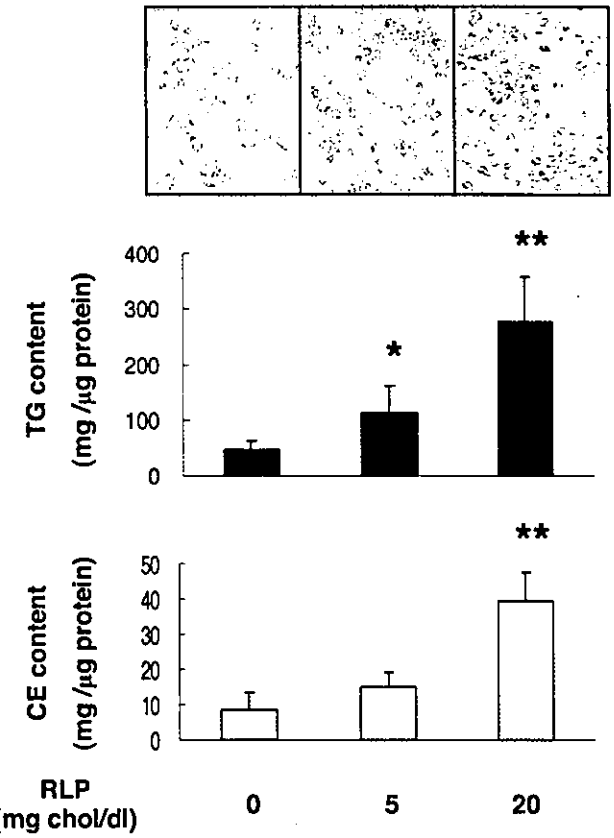

Figure 1. RLPs induce foam cell formation in THP-1 macrophages. THP-1 macrophages were incubated in the presence of RLPs at the indicated concentrations for 24 hours. Photos are representative oil red O staining results of 3 separate experiments. Bar graphs show cellular lipid contents in THP-1 macrophages (n=4). *$P<0.05$. **$P<0.01$ vs 0 mg cholesterol/dL.

differentiation process (Figure 2A) and was not downregulated by incubation with RLPs (Figure 2B).

siRNA Against ApoB48R Decreases RLP-Induced Foam Cell Formation in THP-1 Macrophages

To elucidate the specific role of apoB48R in RLP-induced foam cell formation, we introduced siRNA against apoB48R into THP-1 macrophages. Transfection of THP-1 macrophages with apoB48R siRNA reduced the expression of apoB48R 48 hours after transfection in an apoB48R siRNA dose-dependent manner. However, apoB48R siRNA did not affect the expression of GAPDH (Figure 3A) or that of CD36 (data not shown). When THP-1 macrophages were transfected with apoB48R siRNA, RLP-induced foam cell formation was significantly reduced (Figure 3B). Next, THP-1 macrophages were incubated with β-VLDL derived from apoE−/− mice, a model ligand of apoE-devoid remnant lipoproteins, because it has been reported that apoB48R takes-up TRLs in an apoE-independent fashion.[7,17] ApoB48R siRNA also reduced macrophage foam cell formation induced by β-VLDL. ApoB48R siRNA was more effective compared with the case of RLP-induced foam cell formation (Figure 3C). These results indicate that apoB48R plays a role, at least in part, in the taking up of RLPs, and that the suppression of apoB48R expression may reduce RLP-induced foam cell formation.

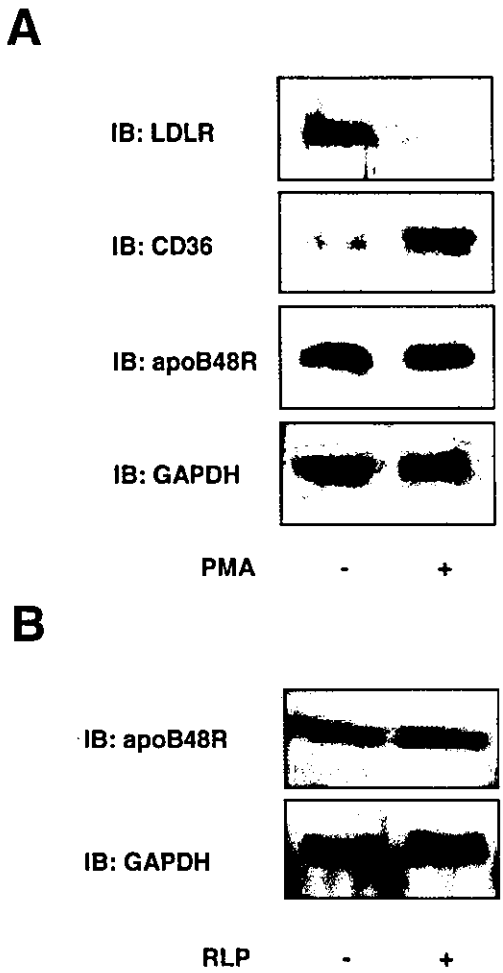

Figure 2. Expression of remnant receptors on THP-1 monocytes and THP-1 macrophages. A, The expression of remnant receptors and related proteins on THP-1 monocytes (PMA−) and THP-1 macrophages (PMA+) were detected with immunoblotting (blots are representative of 3 separate experiments). B, The expression of apoB48R on THP-1 macrophages was detected with immunoblotting before (−) and after (+) RLP treatment (20 mg cholesterol/dL, 24 hours) (blots are representative of 3 separate experiments).

Pitavastatin Inhibits RLP-Induced Foam Cell Formation in THP-1 Macrophages

To examine the effect of pitavastatin on RLP-induced foam cell formation, THP-1 macrophages were incubated with or without pitavastatin for 24 hours. THP-1 lipid contents, very low at baseline, were not significantly affected by treatment with pitavastatin (data not shown). Further, when THP-1 macrophages were pretreated with pitavastatin before RLP treatment, foam cell formation, detected by oil red O staining, was significantly inhibited, and the increments of intracellular TG and cholesterol ester content by RLPs were also significantly reduced by pretreatment with pitavastatin in a dose-dependent manner (Figure 4A).

Pitavastatin Suppresses ApoB48R Expression in THP-1 Macrophages Through RhoA-Dependent Mechanism

Next, we examined whether pitavastatin modulates the expression levels of apoB48R in the THP-1 macrophages. The

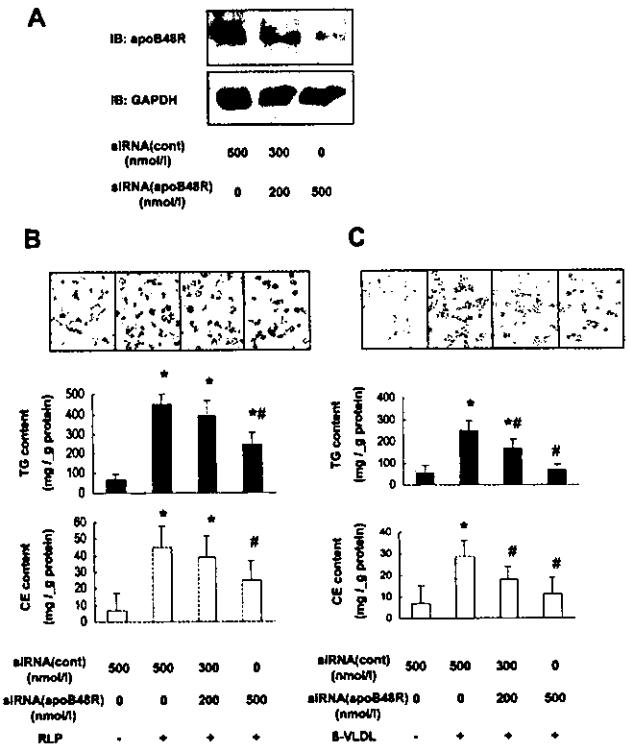

Figure 3. siRNA against apoB48R significantly decreases RLP-induced foam cell formation in THP-1 macrophages. A, THP-1 macrophages were transfected with apoB48R siRNA or control siRNA at the indicated final concentrations, as described in Methods. Forty-eight hours after transfection, the expression of apoB48R was detected with immunoblotting (blots are representative of 3 separate experiments). B, THP-1 macrophages were transfected as in A, and 48 hours after transfection, they were incubated with (+) or without (−) RLP (20 mg chol/dl, 24 hours). Photos are representative oil red O staining results of 3 separate experiments. Bar graphs show cellular lipid contents in THP-1 macrophages (n=4). *P<0.05 vs siRNA (cont) 500 nmol/l, siRNA (apoB48R) 0 nmol/l, RLP (−); #P<0.05 vs siRNA (cont) 500 nmol/l, siRNA (apoB48R) 0 nmol/l, RLP (+). C, THP-1 macrophages were transfected as in A, and 48 hours after transfection, they were incubated with (+) or without (−) β-VLDL (20 mg chol/dl, 24 hours). Photos are representative oil red O staining results of 3 separate experiments. Bar graphs show cellular lipid contents in THP-1 macrophages (n=4). *P<0.05 vs siRNA (cont) 500 nmol/l, siRNA(apoB48R) 0 nmol/l, β-VLDL (−); #P<0.05 vs siRNA (cont) 500 nmol/l, siRNA (apoB48R) 0 nmol/l, β-VLDL (+).

expression level of apoB48R was significantly decreased after 24 hours of incubation with pitavastatin in a dose-dependent manner (Figure 5A). Statins are known to inhibit the mevalonate pathway, resulting in inhibition of the activity of RhoA, a Rho GTPase family member. Many studies have reported that statins exert their bioactive effects via inhibition of RhoA, independent of a lipid-lowering effect. Thus, we examined whether RhoA is involved in the reduction of apoB48R expression by pitavastatin. When THP-1 macrophages were pretreated with GGPP before pitavastatin treatment, reduction of apoB48R expression by pitavastatin was almost restored. In contrast, FPP was not so effective in recovering apoB48R expression compared with GGPP (Figure 5B). To examine whether pitavastatin treatment had an effect on RhoA activity, the GTP-binding capacity of RhoA was measured in THP-1 macrophages. As shown in Figure 5C, the amount of GTPγS-bound RhoA was reduced when

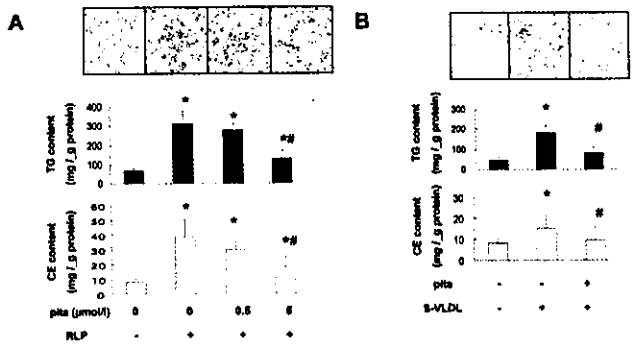

Figure 4. Pitavastatin inhibits RLP-induced foam cell formation in THP-1 macrophages. A, THP-1 macrophages were preincubated in the presence of pitavastatin (pita) at the indicated concentrations for 24 hours and then incubated with (+) or without (−) RLP (20 mg chol/dl, 24 hours). Photos are representative oil red O staining results of 3 separate experiments. Bar graphs show cellular lipid contents in THP-1 macrophages (n=4). *P<0.01 vs pita 0 μmol/l, RLP (−); #P<0.05 vs pita 0 μmol/l, RLP (+). B, THP-1 macrophages were preincubated in the presence (+) or absence (−) of pitavastatin (pita, 5 μmol/l, 24 hours) and then incubated with (+) or without (−) β-VLDL (20 mg chol/dl, 24 hours). Photos are representative oil red O staining results of 3 separate experiments. Bar graphs show cellular lipid contents in THP-1 macrophages (n=4). *P<0.05 vs pita (−), β-VLDL (−); #P<0.05 vs pita (−), β-VLDL (+).

THP-1 macrophages were treated with pitavastatin. Pitavastatin also decreased membrane translocation of RhoA in THP-1 macrophages (data not shown). In addition, C3 exoenzyme, a specific RhoA inhibitor, reduced apoB48R expression in THP-1 macrophages (Figure 5D) and inhibited RLP-induced foam cell formation (Figure 5E). Pitavastatin treatment did not affect the expression of LDL receptor and LRP in THP-1 macrophages (data not shown). Although pitavastatin suppressed CD36 expression by 15% at 5 μmol/L (data not shown), the reduction rate was much lower than that of apoB48R.

Pitavastatin Suppresses ApoE-Deficient β-VLDL Uptake by THP-1 Macrophages

To further confirm whether the inhibition of RLP-induced foam cell formation by pitavastatin is dependent on apoB48R, we examined the effect of pitavastatin on the uptake of β-VLDL derived from apoE−/− mice. THP-1 macrophages were incubated with apoE-deficient β-VLDL in the presence or absence of pitavastatin, and then lipid accumulation was evaluated. These β-VLDL induced macrophage foam cell formation, although to a lesser extent when compared with native RLPs. Consistent with the effect of pitavastatin on apoB48R expression, pretreatment with pitavastatin reduced lipid accumulation in THP-1 macrophages (Figure 4B), supporting the notion that this compound may serve to reduce lipid accumulation even in the absence of apoE-dependent pathway.

Pitavastatin Suppresses ApoB48R Expression in Human Peripheral Blood Macrophages

To demonstrate the involvement of apoB48R in RLP uptake and its potential regulation by pitavastatin in more pathophysiological conditions, we conducted experiments using human peripheral blood macrophages. Western blot analysis showed that pitavastatin treatment for 24 hours significantly reduced